

## Improved performance of oxidized Alizarin based Quasi solid state Dye Sensitized solar cell by Surface Treatment

Manmeeta<sup>1</sup>, Saxena Dhiraj<sup>2</sup>, Sharma G.D.<sup>3</sup> and Roy M.S.<sup>4</sup>

<sup>1</sup>Faculty of Science, National Law University, Jodhpur, Raj., INDIA

<sup>2</sup>Lachoo Memorial College of Science & Technology, Jodhpur, Raj., INDIA

<sup>3</sup>Jaipur Engineering College, Kukas, Jaipur, Raj., INDIA

<sup>4</sup>Defense Laboratory, Jodhpur, Raj., INDIA

Available online at: [www.isca.in](http://www.isca.in)

(Received 22<sup>nd</sup> December 2011, revised 14<sup>th</sup> January 2012, accepted 17<sup>th</sup> January 2012)

### Abstract

The effect of the  $TiCl_4$  (titanium tetrachloride) post-treatment on nanocrystalline  $TiO_2$  films in quasi solid state dye sensitized solar cells (DSSCs) is investigated and compared to nontreated films. DSSCs are fabricated employing metal free oxidized alizarin dye as photo sensitizer, polymer sol gel as electrolyte with PEDOT:PSS coated FTO as counter electrode. The performance of both  $TiCl_4$  treated and nontreated DSSCs are analyzed by cyclic voltammograms, optical absorption spectra, kelvin probe scanning, electrochemical impedance spectra, current-voltage characteristics in dark and under illumination. As a result of this post-treatment, a significant increase in conversion efficiency and short circuit current density is observed. The overall power conversion efficiency improves from 3.57 % to 5.12 % upon  $TiCl_4$  treatment. This improvement is attributed to increase in dye loading, enhancement in electron lifetime and shift in the conduction band edge upon  $TiCl_4$  treatment. Here, the shift in the conduction band edge of the  $TiO_2$  upon  $TiCl_4$  treatment creates a driving force for charge transfer from the LUMO of the dye molecules to the conduction band of  $TiO_2$  which results in improved charge injection.

**Keywords:** Dye sensitized solar cells (DSSCs), kelvin probe studies, dye binding sites, titanium tetrachloride treatment.

### Introduction

The present energy and environment crisis has stimulated the interest in exploring renewable energy sources. In this context, dye sensitized solar cells (DSSCs) based on nanocrystalline  $TiO_2$  certainly appear as one of the most promising candidate as low cost alternative to conventional semiconductor solar cells<sup>1,2</sup>. Since their breakthrough in 1991 as reported by Gratzel et.al<sup>1</sup>, the DSSCs have been attracting a significant attention of the researchers due to their substantial possibilities to fabricate low-cost, environmental friendly, large-area photovoltaic devices. These cells are composed of a wide band gap semiconductor (like  $TiO_2$ , ZnO) deposited on a transparent conducting substrate, an anchored molecular sensitizer, a redox electrolyte ( $I^-/I_3^-$  couple) and a counter electrode<sup>1,3-6</sup>. DSSCs based on Ru-complex photo sensitizers, such as  $N_3$ ,  $N_{719}$  and black dyes have shown high PCE<sup>7-9</sup>. In recent years, metal free organic dyes have been explored as an alternative to Ru-complexes because of low material costs, ease of synthesis and high molar extinction coefficients<sup>10,14-16</sup>. Although DSSCs based on metal free organic dyes as sensitizers, with considerably good efficiencies have been reported<sup>11-13</sup>, yet there is a need to optimize their chemical and physical properties for improving device performance. Extensive research is being carried out to optimize the factors for improving the efficiency of DSSCs, such as enhanced diffusion of dye, choice of electrodes and optimization of electrolytes etc.

Extent of diffusion of dye into nano-crystalline  $TiO_2$  matrix significantly affects efficiency and photocurrent in DSSCs. The electron transport at the dye / nanocrystalline semiconductor interface is a key step in the energy conversion process as photo excited electrons in dye molecules are transferred to an external circuit through this semi conductor film. Electron transport is sensitive to the structure of the dye since electrons passes through its overlapping molecular orbitals and semi-conductor surface. Electron transport process is also affected by how and where the dye is adsorbed over the surface.

Extent of diffusion of dye into nano-crystalline  $TiO_2$  matrix significantly affects efficiency and photocurrent in DSSCs. There are various methods to increase the dye diffusion into  $TiO_2$  matrix. One of such significant method is titanium tetrachloride ( $TiCl_4$ ) post-treatment of the  $TiO_2$  film. The  $TiCl_4$  surface treatment causes improvement in electron transport and dye anchoring, resulting in enhanced efficiency for the solar cells<sup>17-21</sup>.

Herein we have investigated and compared the performance of DSSCs based on untreated and  $TiCl_4$  treated  $TiO_2$  electrodes. DSSCs have been fabricated using both  $TiCl_4$  treated and untreated -nanoporous  $TiO_2$  films as base electrodes, oxidized alizarin dye as photo sensitizer, polymer sol gel as electrolyte and PEDOT:PSS coated FTO as counter electrode.

The performance of both  $\text{TiCl}_4$  treated and untreated DSSCs are analyzed by cyclic voltammograms, optical absorption spectra, electrochemical impedance spectra, current–voltage characteristics in dark and under illumination. We observed a significant increase in incident photon to current conversion efficiency (IPCE) and short circuit current density ( $J_{sc}$ ) upon  $\text{TiCl}_4$  treatment as compared to untreated films. We have also carried out Kelvin probe scanning to study the variation in surface potential upon  $\text{TiCl}_4$  treatment. The overall power conversion efficiency improves from 3.57 % and 5.12 % upon  $\text{TiCl}_4$  treatment. This improvement is attributed to increase in dye loading, enhancement in electron lifetime and shift in the conduction band edge upon  $\text{TiCl}_4$  treatment. Here, the shift in the conduction band edge of the  $\text{TiO}_2$  upon  $\text{TiCl}_4$  treatment creates a driving force for charge transfer from the LUMO of the dye molecules to the conduction band of  $\text{TiO}_2$  which results in improved charge injection.

## Material and Methods

**Preparation of photo-electrodes:** Fluorine doped Tin Oxide (FTO) glass plates were cleaned in detergent solution, rinsed with de-ionized water and acetone and dried in ambient conditions. A  $\text{TiO}_2$  colloidal dispersion was prepared by adding 6gm of  $\text{TiO}_2$  ( $\text{P}_{25}$  Degussa product) powder in 2 ml of distilled water. Further, 0.2ml of acetyl acetone (particle stabilizer) was added to prevent the re-aggregation of  $\text{TiO}_2$  particles. Finally 8.0ml of distilled water and 0.1ml of Triton X-100 (to lower the surface tension of the colloid in order to facilitate easier spreading onto the conducting glass plate) were slowly added with continuous mixing for 10 min. A plastic adhesive tape was fixed as spacer on the three sides of conducting glass substrate (FTO) to restrict the area and thickness of  $\text{TiO}_2$  film. A plastic adhesive tape was fixed as spacer on the three sides of conducting glass substrate (FTO) to restrict the area and thickness of  $\text{TiO}_2$  film. The prepared colloidal paste of  $\text{TiO}_2$  was spread over FTO substrate employing Doctor Blade technique to obtain a nanocrystalline layer. After the  $\text{TiO}_2$  layers get dried, the films were sintered at  $450^\circ\text{C}$  for 30 minutes in air to improve the electronic contact among particles and to burnout organic binders.

**$\text{TiCl}_4$  Post Treatment:** Freshly sintered  $\text{TiO}_2$  film was treated with  $\text{TiCl}_4$  employing the method as described in literature<sup>20</sup>. For post-treatment with  $\text{TiCl}_4$ , an aqueous stock solution of 2 M  $\text{TiCl}_4$  was diluted to 0.05 M. Sintered  $\text{TiO}_2$  film was immersed into this solution in an air tight closed glass vessel for 24 hours and then was taken out and dried.

**Dye Sensitization of photo electrodes:** We have oxidized standard alizarin dye in alkaline medium. Solution of oxidized alizarin dye was prepared in methanol. UV-Visible absorption spectra of alizarin (oxidized) was recorded using a Perkin Elmer spectrophotometer (F-4500 model). The sensitization of  $\text{TiCl}_4$  treated  $\text{TiO}_2$  and untreated  $\text{TiO}_2$  electrodes were carried out by overnight immersion in

methanol solution containing  $5 \times 10^{-4}$  M of oxidized alizarin at room temperature. Films were washed again with the solution and were allowed to dry for 30 min. UV–visible absorption spectra was recorded for both dye sensitized untreated  $\text{TiO}_2$  electrode and dye sensitized  $\text{TiCl}_4$  treated  $\text{TiO}_2$  electrode by a Perkin Elmer spectrophotometer (F-4500 model). Kelvin Probe studies were also carried out for both dye sensitized untreated and  $\text{TiCl}_4$  treated  $\text{TiO}_2$  electrodes employing SKP Kelvin Probe (SKP 4.5) to obtain 3-D work function imaging. The cyclic voltammetry measurements were done with a potentio-stat (Auto-Lab model), at room temperature using a three-electrode system.

**Fabrication of dye sensitized solar cells and their characterization:** A quasi solid state polymer electrolyte was prepared by mixing LiI (0.1 g), I<sub>2</sub> (0.019 g), propylene carbonate (5 mL),  $\text{P}_{25}$   $\text{TiO}_2$  (0.0383 g), PEO (0.2648 g), and 4-tert-butylpyridine (0.044 mL) into acetonitrile (5 mL) solvent as reported in literature.  $\text{TiO}_2$  ( $\text{P}_{25}$  Degussa) powder was added as nano-fillers in the polymer electrolyte. This electrolyte was then spread over the dye sensitized photo electrodes by spin coating method to form the hole transporting layer. The counter electrodes were made by developing a thin film of protonated poly-(3,4-ethylenedioxythiophene)-polystyrene (PEDOT:PSS) over graphite coated FTO glass substrates. In this process, first the FTO is coated with graphite and then DMSO treated PEDOT:PSS was grown over the top of the film by spin coating method. The counter electrode was allowed to dry at  $80^\circ\text{C}$  for 30 min. The DSSCs were made by clamping the photoelectrode consisting of polymer electrolyte with counter electrode. We have fabricated quasi solid state DSSCs with following configurations: FTO/ $\text{TiO}_2$ –Alizarin (oxidized)/polymer electrolyte/PEDOT:PSS coated FTO (*device A*), FTO/ $\text{TiCl}_4$  treated  $\text{TiO}_2$  –Alizarin (oxidized) /polymer electrolyte /PEDOT:PSS coated FTO (*device B*).

The current–voltage (J–V) characteristics in dark and under illumination were recorded by a Keithley electrometer with built in power supply. The Electrochemical Impedance Spectra (EIS) measurements were carried out by applying bias of the open circuit voltage ( $V_{oc}$ ) and recorded over a frequency range of 1mHz to  $10^5$  Hz with AC amplitude of 10mV. The above measurements were recorded with an Autolab Potentiostat PGSTAT-30 equipped with frequency response analyzer (FRA).

## Results and Discussion

**Electrochemical and Optical characterization of dye:** The energetic alignment of highest occupied molecular orbital (HOMO) and lowest unoccupied molecular orbital (LUMO) energy levels of sensitizer is crucial for efficient operation of DSSC. To ensure efficient electron injection from the excited state into the conduction band edge of  $\text{TiO}_2$  films, the LUMO level of the sensitizer must be higher in energy than the  $\text{TiO}_2$

conduction band edge. The HOMO level of the sensitizer must be lower in energy than the redox potential of the  $I/I_3^-$  redox couple for efficient regeneration of the dye cation after photoinduced electron injection into the  $TiO_2$  film. The electrochemical behavior of the alizarin (oxidized) dye was investigated by cyclic voltammetry. The CV graph of alizarin (oxidized) is shown in figure 1. The oxidation potential ( $E_{ox}$ ) and reduction potential ( $E_{red}$ ) have been measured with respect to the  $Ag/Ag^+$  electrode. HOMO and LUMO levels were calculated from the following equations<sup>35</sup>.  $E_{HOMO}$  (eV) = - e [ $E_{ox}$  (V) + 4.4],  $E_{LUMO}$  (eV) = - e [ $E_{red}$  (V) + 4.4]

The values of HOMO and LUMO are summarized in the table 1. The HOMO – LUMO levels of the dye are suitable for DSSCs efficient operation. The LUMO energy level ( - 3.25 eV) is sufficiently higher than the conduction band edge of  $TiO_2$  ( - 4.1 eV ). Hence, an effective electron transfer from the excited dye to  $TiO_2$  film is ensured. The HOMO level of dye (-5.23 eV) is about 0.4 eV lower in energy than the redox potential of redox couple (-4.83 eV vs vacuum)<sup>12</sup>, and thus a sufficient driving force for the regeneration of oxidized dye is available.

**Table 1**  
**Optical and electrochemical properties of Dye**

Dye	Alizarin	Alizarin (Oxidized)
$\lambda_{max}$ in solution (nm)	430	540
$E_g^{opt}$ (eV)	2.2	1.90
HOMO (eV)	-	-5.23
LUMO(eV)	-	-3.25
$E_g^{el}$	-	1.98

Figure 2 presents the normalized UV-vis absorption spectra of both alizarin dye and alizarin dye (oxidized). Alizarin dye and alizarin dye (oxidized) exhibit different absorption bands 400 -500 nm (in the visible range) and 480-650 nm (in extendable visible range) respectively as shown in figure 2. The red shift in the absorption spectra of alizarin dye (oxidized) has been attributed to increase in the conjugation length, which in fact reduces the optical band gap of the dye. This shifting indicates a greater electron delocalization in alizarin (oxidized) as compared to pure dye. The optical band gap ( $E_g^{opt}$ ) of alizarin dye (oxidized) as determined from its absorption data is about 1.9 eV. The value of energy band gap ( $E_g^{el}$ ) was estimated through the analysis of the electrochemical data and was found quite close to optical band gap ( $E_g^{opt}$ ) as extrapolated from the absorption onset. This demonstrates the reliability of the electrochemical evaluation of the LUMO and HOMO levels.

**Characterization of electrodes:** Figure 3 shows the UV-visible spectra of dye sensitized untreated and  $TiCl_4$  treated  $TiO_2$  electrodes. In comparison to the spectrum of oxidized dye in solution, the absorption spectrum of both dye sensitized treated and untreated  $TiO_2$  films were broadened, indicating substantial absorption of dye molecules on the  $TiO_2$  surface. The broadening of absorption spectra is due to interaction between the dye and  $TiO_2$ . The absorption spectra

also reveal that there is almost constant increase in absorption throughout visible region due to  $TiCl_4$  treatment of nanocrystalline  $TiO_2$  surface. It may be interpreted that this treatment increases porosity of the surface and this surface modification apparently increases the amount of adsorbed dye molecules. As the absorption coefficient of the dye sensitized  $TiCl_4$  treated  $TiO_2$  photoelectrode has been significantly increased as compared to dye sensitized untreated  $TiO_2$  electrode, it indicates that there is a substantial increase in absorption of dye due to surface treatment by  $TiCl_4$ . To estimate the relative increase in dye loading, we have carried out dye de-sorption experiment on untreated and treated  $TiO_2$  films as described in literature<sup>9</sup>. For both treated and untreated  $TiO_2$  films, dye was desorbed from the electrodes by treating with a quantified amount of diluted  $NH_3$  in water, resulting in a dye solution of which a UV /VIS spectrum has been recorded. The relative difference in absorbance may be directly translated into the relative difference in dye loading of the  $TiO_2$  surface as the absorbance is linearly related to the concentration of dye. The difference in absorbance between  $TiCl_4$ -treated and untreated  $TiO_2$  is distinctive, showing almost 18% higher dye loading for  $TiCl_4$ -treated electrodes.

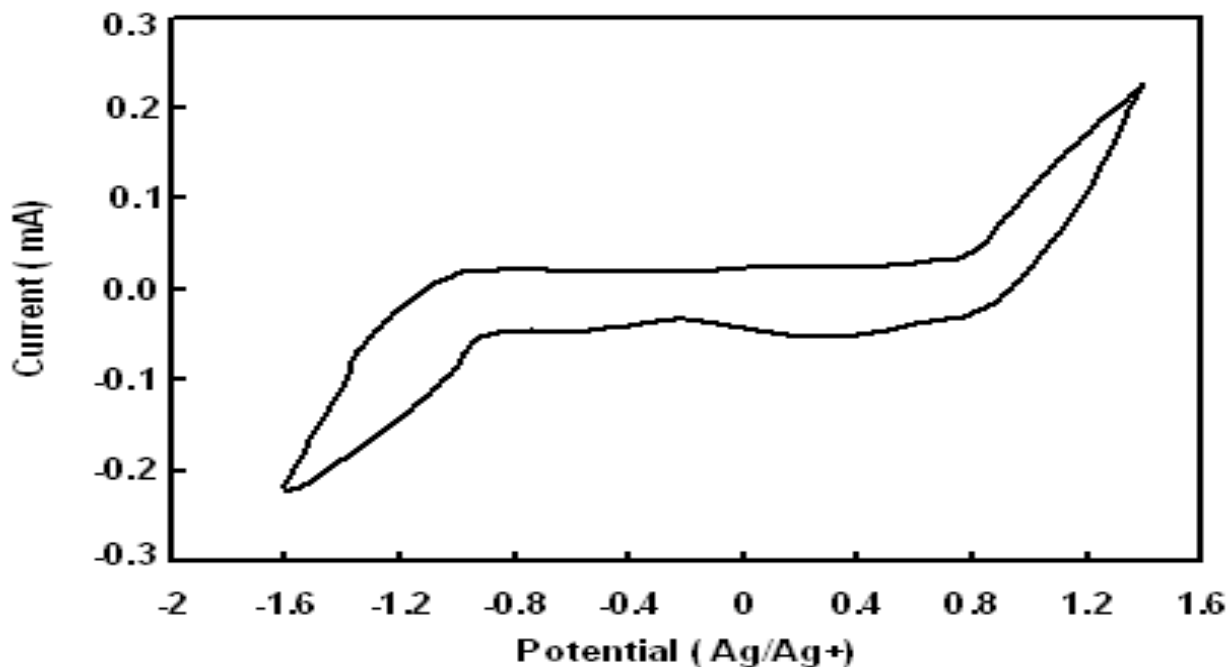
The Kelvin Probe technique is an established direct, noncontact method in semiconductor surface electronics to determine the work function of a (semi) conducting solid. This technique is also used for determination of surface potential of organic mono-layer on solid substrates and to evaluate effect of adsorbents on work function. The work function can be directly correlated to the surface condition.

Figure 4(a) and 4(b) shows screenshots of work function difference chart of untreated and  $TiCl_4$  treated  $TiO_2$  electrodes sensitized with dye as obtained using Kelvin Probe scanning. Backing voltage  $V_b$  is ranging from -7000 mV to 7000 mV in both the cases covering 100 points. Work function for dye sensitized untreated  $TiO_2$  electrode and  $TiCl_4$  treated  $TiO_2$  electrode is obtained as - 4.711 eV and - 4.659 eV, respectively. This change in work function indicates a shift in the Fermi level of the  $TiO_2$  upon  $TiCl_4$  treatment.

**Current–Voltage characteristics:** The J–V characteristics of device A and device B, under the illumination intensity of 100 mW/cm<sup>2</sup> are shown in figure 5(a). The photovoltaic parameter, i.e. short circuit current ( $J_{sc}$ ), open circuit voltage ( $V_{oc}$ ), fill factor (FF) and power conversion efficiency ( $\eta$ ) as estimated from these curves are compiled in Table 2. Obtained data indicates an improvement in all the photovoltaic parameters upon  $TiCl_4$  treatment. The value of overall power conversion efficiency i.e. 3.57% for device A based on untreated  $TiO_2$  electrode increases to 5.12% upon  $TiCl_4$  treatment in device B. The  $J_{sc}$  of DSSCs is mainly influenced by the sensitizer (dye) loading and the electron transfer efficiency in the  $TiO_2$  film<sup>33</sup>.

**Table-2**  
**Photovoltaic parameters of the quasi solid state dye sensitized solar cells**

Device	Short circuit current ( $J_{sc}$ ) (mAcm <sup>-2</sup> )	Open circuit voltage ( $V_{oc}$ ) (V)	Fill factor (FF)	Power conversion efficiency ( $\eta$ ) (%)
A	9	0.75	0.53	3.57
B	11.2	0.80	0.58	5.12



**Figure-1**  
 Cyclic voltammograms of Alizarin dye (oxidized)

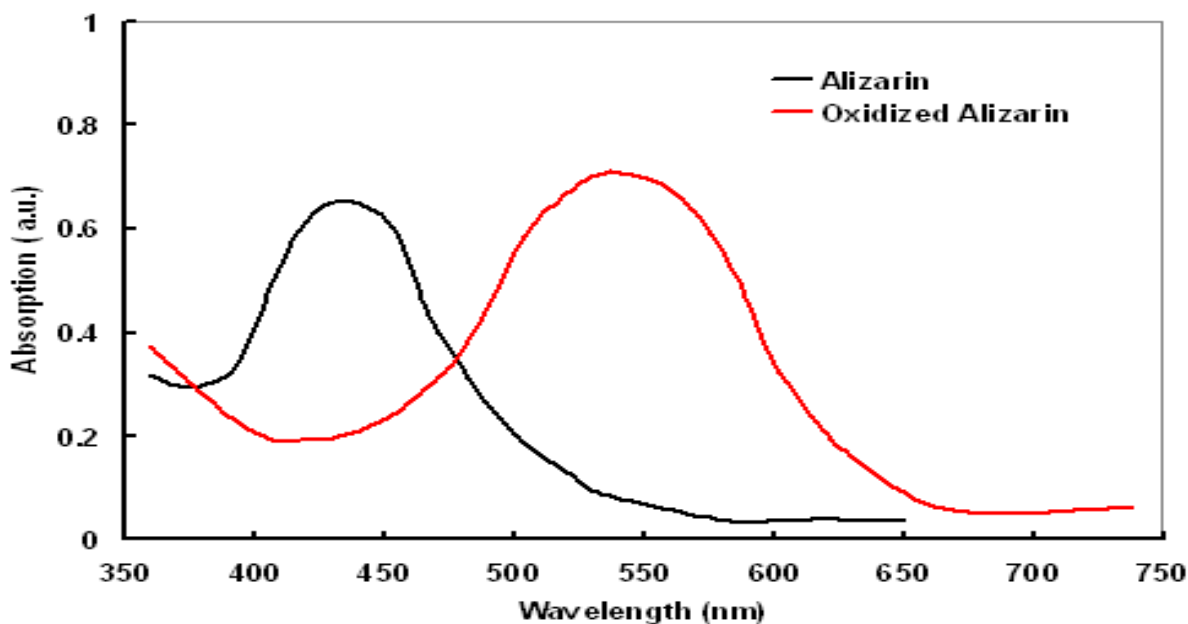


**Figure-2**  
 Normalized UV-Visible absorption spectra of Alizarin and Alizarin dye (oxidized)

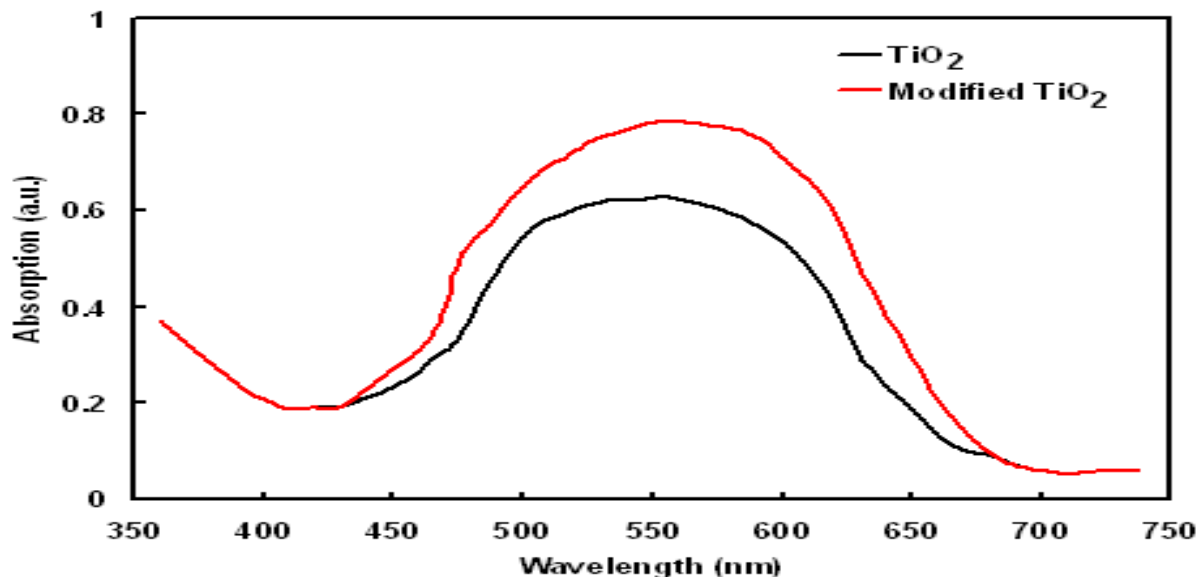
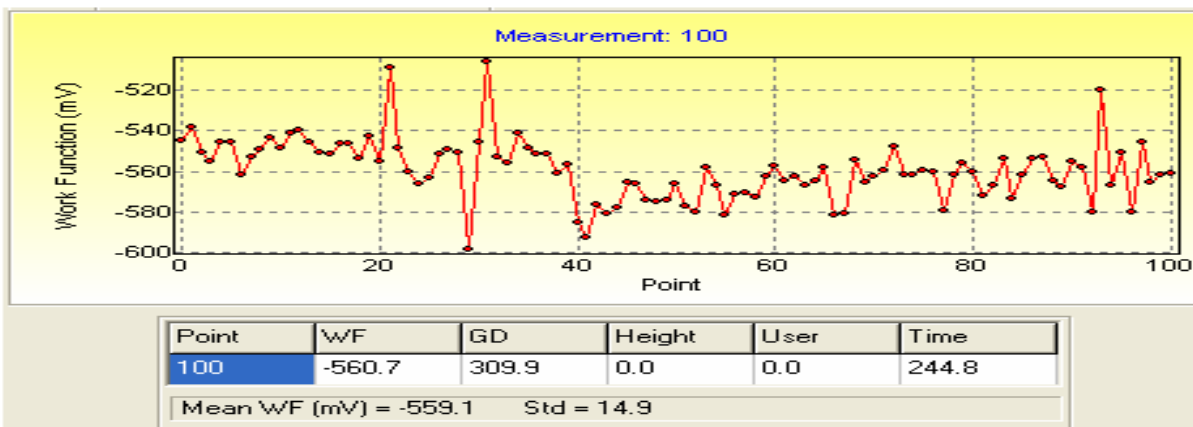
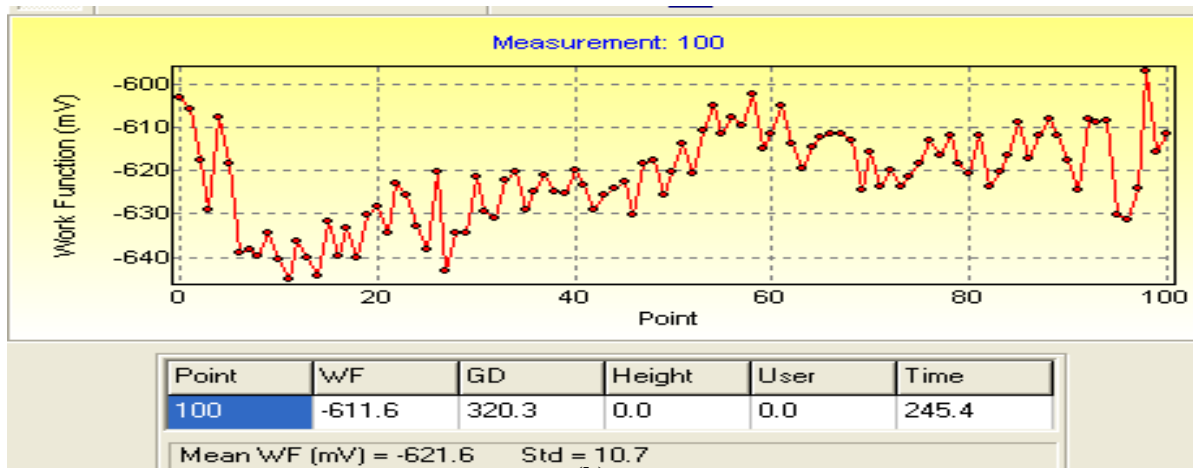


Figure-3

Normalized UV-Visible absorption spectra of Alizarin (oxidized) adsorbed on untreated and  $\text{TiCl}_4$  treated  $\text{TiO}_2$  electrodes



(a)



(b)

Figure-4

Work function charts for (a) untreated  $\text{TiO}_2$  and (b)  $\text{TiCl}_4$  treated  $\text{TiO}_2$  sensitized with dye

The dye loading for treated TiO<sub>2</sub> electrode is about 18 % higher than that for untreated TiO<sub>2</sub> electrode, therefore the increase in dye loading may be considered as one of the significant factor for the increase in J<sub>sc</sub>. TiCl<sub>4</sub> treatment provides additional adsorption sites for the dye on TiO<sub>2</sub> surface resulting in increased dye loading which in turn causes an increase in J<sub>sc</sub>.

The V<sub>oc</sub> in DSSCs is directly related with the concentration of electrons injected from the LUMO of the dye to the conduction band of TiO<sub>2</sub>. The V<sub>oc</sub> is mainly limited by the recombination of conduction band electrons with the I<sub>3</sub><sup>-</sup> ions present in the electrolyte and also to the oxidized sensitizer. Since the dye loading is more for the TiCl<sub>4</sub> treated electrode, we consider that the concentration of electrons in the conduction band of treated TiO<sub>2</sub> electrode is high, which leads to an increase in the V<sub>oc</sub>. We also assume that a compact layer is formed in the treated TiO<sub>2</sub> electrode, supporting the accumulation of electrons at the surface of FTO, which results in the negative shift in Fermi level and eventually produces a larger value of V<sub>oc</sub><sup>23</sup>.

The back electron transfer, i.e. electron leakage, which is the origin of the dark current, plays an important role in the photovoltaic performance of DSSCs<sup>20,24</sup>. The reduction of electron leakage is necessary to enhance the power conversion efficiency of DSSCs. The dark current measurement provides valuable information regarding back electron transfer process in DSSCs.

The effect of TiCl<sub>4</sub> treatment is further confirmed by the J-V characteristics in dark as shown in figure 5(b). The origin of dark current in DSSC is due to the porous nature of TiO<sub>2</sub> structure, which provides pathways for liquid redox electrolyte (i.e. I<sub>3</sub><sup>-</sup> species) to penetrate through the porous film and contact the FTO surface. During the penetration, electron recombination takes place and causes reduction in photocurrent. It can be seen from this figure that the dark current decreases upon TiCl<sub>4</sub> treatment (in device B) as compared to the untreated device (in device A). It is also observed that the TiCl<sub>4</sub> treatment shifts the onset potential towards higher potential (from 0.40V to 0.52 V). The increase in the onset potential and reduction in the dark current upon TiCl<sub>4</sub> treatment reduces the uncovered surface area of FTO surface by forming a blocking layer and also reduces the back electron transfer. The observed decrease in dark current is a result of the suppression of I<sub>3</sub><sup>-</sup> reduction at the dye sensitized TiO<sub>2</sub> electrode<sup>25</sup>, and consequently results in an enhancement in the photovoltaic performance. To carry out detailed analysis of improved photovoltaic performance upon TiCl<sub>4</sub> treatment, IPCE measurements have been carried out. The Incident Photon to Current Efficiency (IPCE) is defined as the ratio of number of photoelectrons in the external circuit as produced by an incident photon at a given wavelength (λ). Value of IPCE may be determined by using following equation:  $IPCE (\%) = 1240 J_{sc} / \lambda P_{in}$

Where J<sub>sc</sub> is the short circuit photocurrent and P<sub>in</sub> is the illumination intensity at wavelength (λ). The IPCE values for device A and device B are determined using this equation and are plotted as a function of illumination wavelength as shown in figure 6. The device B shows higher IPCE values than that of device A as a result of TiCl<sub>4</sub> treatment. IPCE of a DSSC is a result of light harvesting efficiency (LHE), charge injection efficiency (φ<sub>inj</sub>), and conversion efficiency (η<sub>cc</sub> %). The relation between these factors is given by the following equation<sup>26</sup>:  $IPCE (\lambda) = LHE (\lambda) \phi_{inj} \eta_{cc}$

Where LHE (λ) is light harvesting efficiency, φ<sub>inj</sub> is the quantum yield of electron injection from the excited state (LUMO) of the sensitizer into the conduction band of the nano-crystalline semiconductor used in photoanode (charge injection efficiency), and η<sub>cc</sub> is the efficiency of the collection of charge carriers at back electrode. The observed increase in IPCE as shown in figure 6 may be attributed to various factors such as LHE, φ<sub>inj</sub> and η<sub>cc</sub>. The factor, LHE is mainly related to TiO<sub>2</sub> surface area, dye loading, and light scattering/reflection. The dye desorption experiments here confirms that the TiCl<sub>4</sub>-treated electrodes adsorb 18% more dye than the nontreated electrodes. This increase in dye adsorption may be attributed to availability of more specific binding sites on the TiO<sub>2</sub> surface upon TiCl<sub>4</sub> treatment. Thus the most obvious fact causing an increase in LHE upon TiCl<sub>4</sub> treatment may be attributed to increased dye adsorption on TiO<sub>2</sub> surface. Potentially, the TiCl<sub>4</sub> treatment also reduces the fraction of the TiO<sub>2</sub> surface area that is inaccessible for the dye due to sterical constraints as reported. This enhanced dye loading being a significant factor to influence the LHE, causes an increase in LHE and thus may be attributed as one of the reasons for the enhancement in IPCE or subsequently J<sub>sc</sub>. Since the factor φ<sub>inj</sub> is related to the energetic discrepancy between the conduction band of TiO<sub>2</sub> and the LUMO level of sensitizer. To understand whether TiCl<sub>4</sub> treatment causes a shift in conduction band edge, we have carried out Kelvin probe studies as reported earlier in this communication. Based on the observations, we have calculated a clear variation in work function of the electrode upon TiCl<sub>4</sub> treatment which indicates a shift in the conduction band edge of the TiO<sub>2</sub> upon TiCl<sub>4</sub> treatment. This shift or energetic difference creates a driving force, which facilitates charge transfer from the LUMO of the dye molecules to the conduction band of TiO<sub>2</sub>. Moreover, this shift also increases quantum efficiency and the rate of electron injection from excited dye into TiO<sub>2</sub>. This causes an obvious increase in J<sub>sc</sub> and IPCE. η<sub>cc</sub> is another important factor which contributes to observed enhancement in IPCE upon TiCl<sub>4</sub> treatment. The charge recombination in the electrode/electrolyte interface causes a loss of electron collection along the TiO<sub>2</sub> layer. TiCl<sub>4</sub> treatment forms a thin barrier layer that delays the recombination reaction and also blocks back flow in the back reaction (tri-iodides of redox electrolyte and cations of dye), which in turn causes an increase in V<sub>oc</sub> and IPCE.

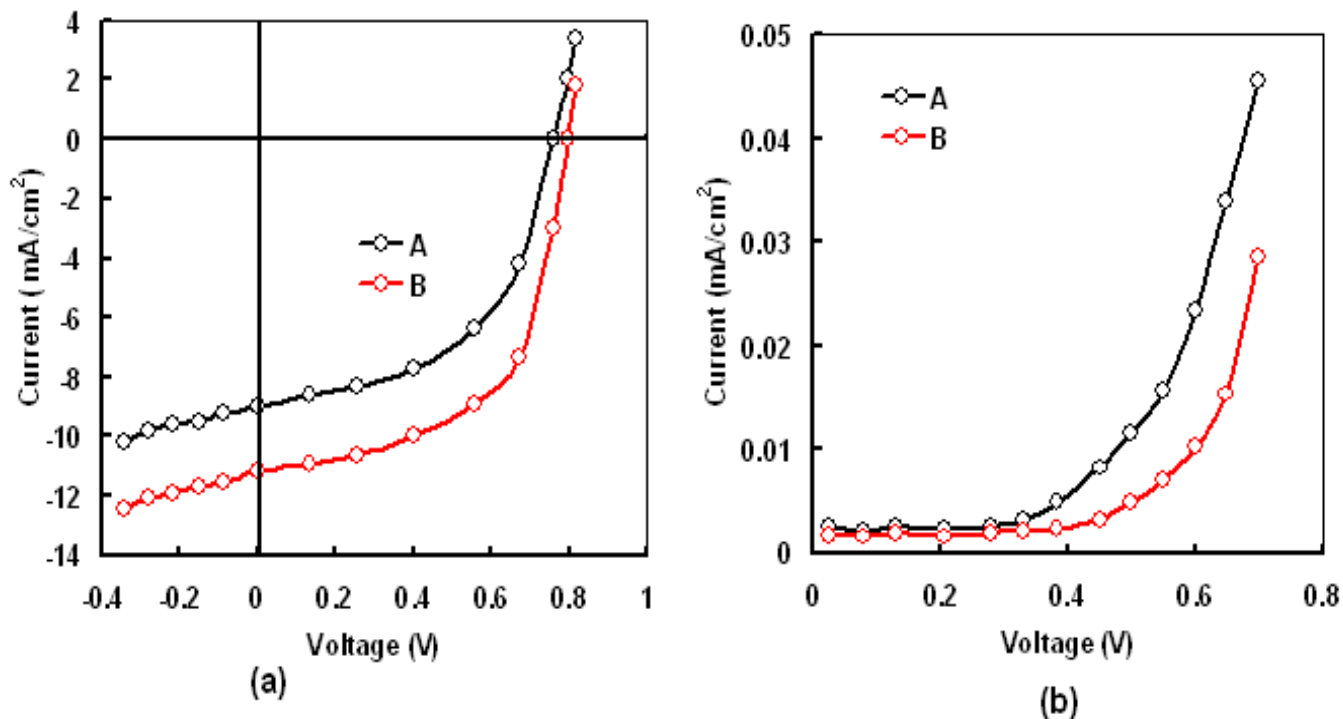


Figure-5

(a) Current –voltage characteristics under illumination and in (b) dark for Quasi solid state DSSCs A and B

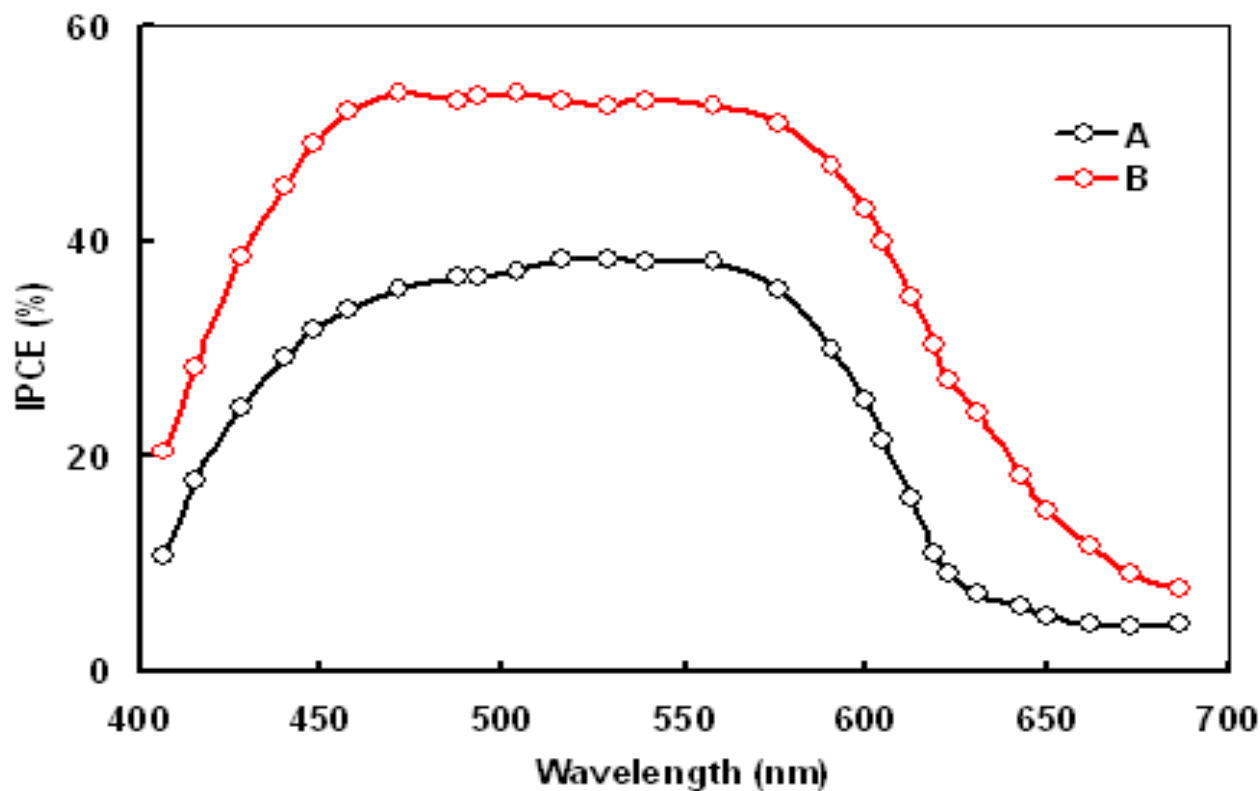


Figure-6

IPCE spectra of Quasi solid state DSSCs A and B

Since the amount of the photogenerated electrons is directly proportional to the incident illumination intensity, the variation of short circuit photocurrent ( $J_{sc}$ ) with the illumination intensity ( $P_{in}$ ) may be used to get information about electron transfer kinetics and also about the amount of photogenerated electrons contributing to photocurrent. Figure 7(a) shows that for both the DSSCs with untreated and  $TiCl_4$  treated  $TiO_2$ ,  $J_{sc}$  is directly proportional to the illumination intensity ( $P_{in}$ ).

Figure 7(a) also shows that the slope for the  $TiCl_4$  treated  $TiO_2$  (0.128) is 39.13 % higher than that for untreated  $TiO_2$  (0.092) electrode. It indicates that 39.13 % more electrons are collected from the same amount of photogenerated electrons at FTO surface upon  $TiCl_4$  treatment. This confirms that  $TiCl_4$  treatment of  $TiO_2$  electrode in DSSCs facilitates electron transfer at the interface, resulting in an increase in collection efficiency.

Open circuit voltage decay (OCVD) technique has been employed as a powerful tool to study the electron lifetime in DSSCs. This technique also provides some quantitative information on the electron recombination rates in DSSCs<sup>27</sup>. In order to conduct the OCVD measurement, the device is illuminated with white light and a steady state voltage is obtained. The decay of voltage is then monitored after interrupting the illumination. The measured decay of the photo voltage reflects a clear decrease in electron concentration at the FTO surface, which is mainly caused by the charge recombination.

Figure 7 (b) shows the OCVD curves of DSSCs based on untreated and  $TiCl_4$  treated  $TiO_2$  electrodes. These curves indicate that the OCVD response of device B ( $TiCl_4$  treated  $TiO_2$ ) is much slower than that of device A (untreated  $TiO_2$ ). From the OCVD measurement, the electron lifetime ( $\tau_n$ ) is determined by the reciprocal of the derivatives ( $dV_{oc}/dt$ ) of the decay curves normalized by the thermal voltage ( $kT/q$ ), using the following expression:  $\tau_n = kT/q (dV_{oc}/dt)$

The value of  $\tau_n$  for the DSSC with  $TiCl_4$  treated  $TiO_2$  film is longer than that for untreated  $TiO_2$  film. It suggests that electron injected from the excited dye can survive for a longer time upon  $TiCl_4$  treatment and hence facilitates electron transport without undergoing losses at FTO surface. Therefore, OCVD measurements demonstrate that due to the longer electron lifetime, the photoelectron recombination rate is reduced effectively upon  $TiCl_4$  treatment of  $TiO_2$ .

**Electrochemical impedance spectra analysis:** The electrochemical impedance spectroscopy has been widely used to investigate the electron transport and the recombination processes in the DSSCs. Figure 8 shows the

EIS spectra of the quasi solid state DSSCs device A and device B. Nyquist plots of these devices are consisting of two semicircles as shown in figure 8(a). The semicircle in high frequency region is attributed to impedance related to charge transport at PEDOT:PSS counter electrode. The large semicircle in low frequency region represents electron transfer at  $TiO_2$ /electrolyte interface and ion diffusion of redox species, in the electrolyte. It can be seen from the figure 8(a) that the diameter of the semicircle corresponds to the device B is higher than that for device A, due to the higher value of charge transfer resistance for device B. This indicates that the recombination of injected electrons with the tri-iodide ions has been reduced upon  $TiCl_4$  treatment in device B as compared to the device A.

The bode plots of the EIS spectra in middle frequency range are shown in figure 8(b). The frequency peak related to the device B shifts towards the lower frequency region as compared to device A. The electron lifetime ( $\tau_n$ ) has been estimated from the expression  $\tau_n = 1/2\pi f_p$ , where  $f_p$  is the peak frequency. It is found that the electron lifetime in device B is higher than device A. The increase in electron lifetime in device B decreases the interfacial recombination for electrons with tri-iodide ions. This may be one of the reasons for the improvement of power conversion efficiency upon  $TiCl_4$  treatment.

## Conclusion

In conclusion, we have reported quasi solid state DSSCs based on  $TiCl_4$  treated and untreated nanoporous  $TiO_2$  electrodes using alizarin dye (oxidized) as photo-sensitizer and PEDOT:PSS coated FTO as counter electrode. The performance of the DSSCs is investigated systematically employing J-V characteristics in dark and under illumination, incident photon to current efficiency (IPCE), OCVD measurements, Kelvin probe scanning and electrochemical impedance spectra measurements. It was found that the PCE significantly improves from 3.57% to 5.12 % upon  $TiCl_4$  treatment. The improvement in the PCE is due to an increase in dye loading or availability of more specific binding sites on the  $TiO_2$  surface upon treatment and also due to reduction in dark current. We have analyzed that  $TiCl_4$  treatment causes a shift in the conduction band edge of  $TiO_2$  which is an important factor responsible for observed increase in the efficiency upon  $TiCl_4$  treatment. Kelvin Probe scanning charts indicate a clear shift in conduction band edge upon  $TiCl_4$  treatment. This shift creates a driving force for charge transfer from the LUMO of the dye molecules to the conduction band of  $TiO_2$ . This improved efficiency has also been attributed to the longer electron lifetime due to  $TiCl_4$  treatment. Due to the longer electron lifetime, the photoelectron recombination rate is reduced effectively upon  $TiCl_4$  treatment of  $TiO_2$ .



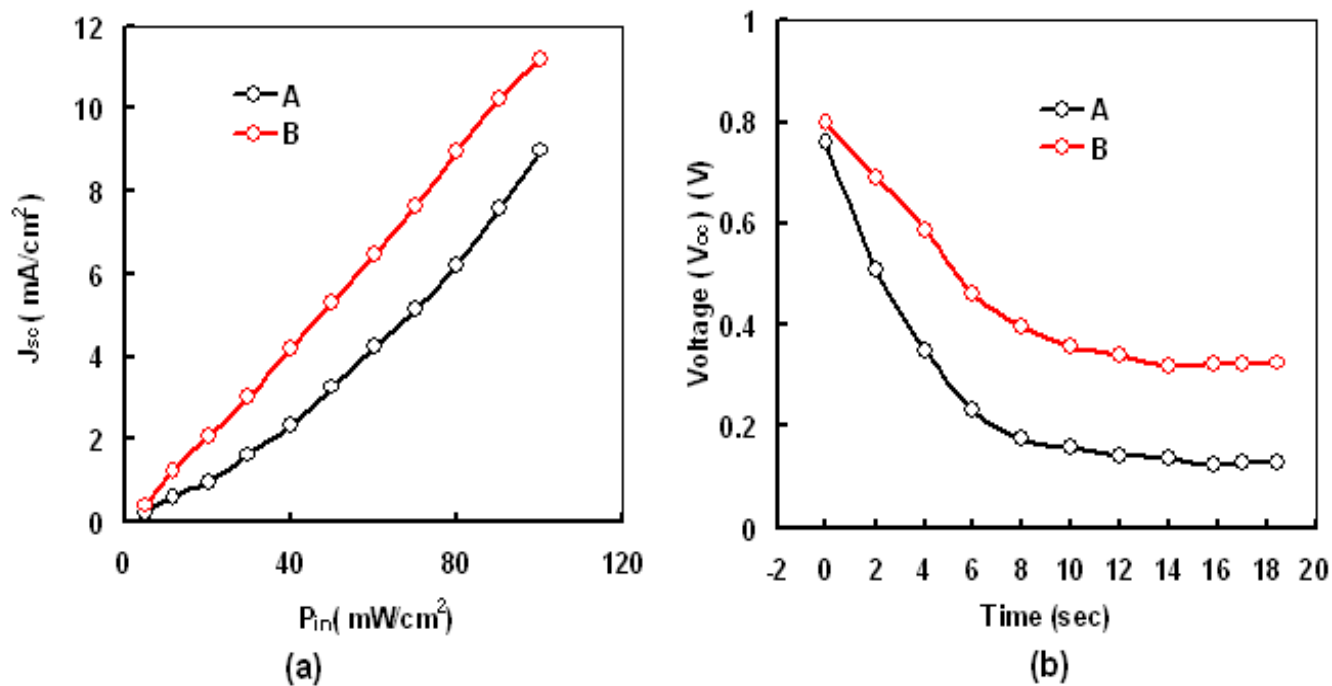


Figure-7

(a) Variation of  $J_{sc}$  with illumination intensity  $P_{in}$  and (b) open circuit voltage decay for Quasi solid state DSSCs A and B

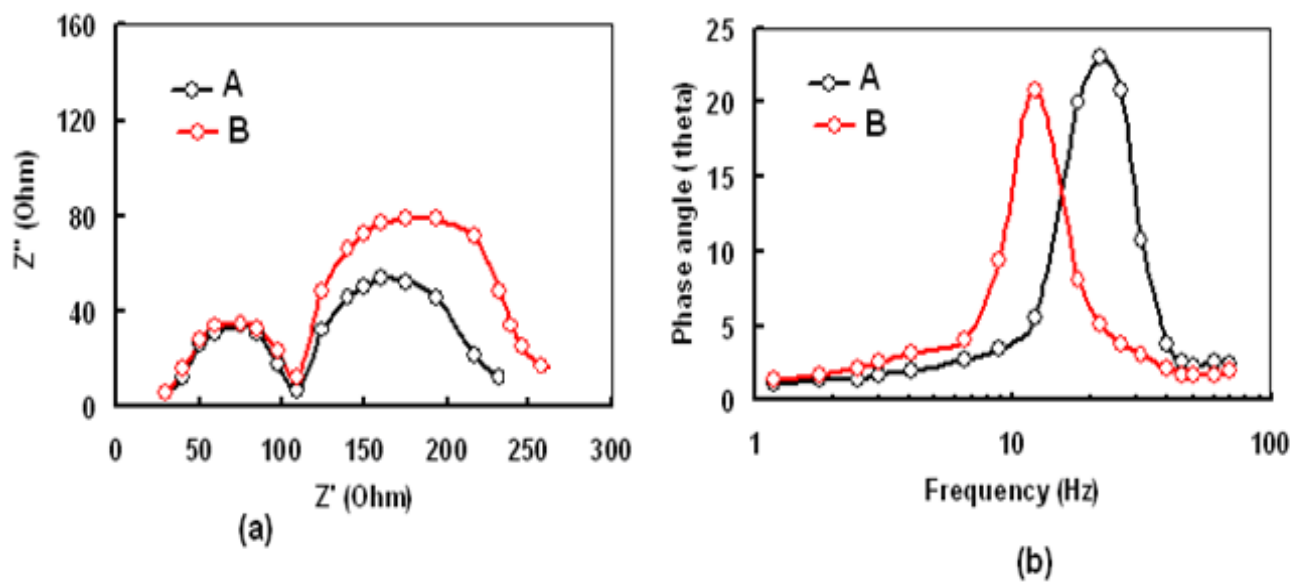


Figure-8

EIS spectra (a) Nyquist plots (b) Bode plots for DSSCs A and B

## References

1. O'Regan B. and Grätzel M., A low cost, high efficiency solar cell based on Dye Sensitized colloidal TiO<sub>2</sub> films, *Nature*, **353**, 737 – 739 (1991)
2. Hagfeldt A. and Gratzel M., Molecular Photovoltaics, *Acc. Chem. Res.*, **33**, 269 (2000)
3. Robertson N., Optimising Dyes for Dye Sensitized Solar Cells, *Angewandte Chem. Int. Edi*, **45**, 2338-2345 (2006)
4. Kippelen B. and Bredas J.L., Organic Photovoltaics, *Energy Environ. Sci.*, **2**, 251 (2009)
5. Barote Maqbul A., Ingale Babasaheb D., Tingre Govind D., Yadav Abhijit A., Surywanshi Rangrao V. and Masumdar Elahipasha U., Some Studies on Chemically Deposited n-PbSe Thin Films, *Res. J. Chem. Sci.*, **1(9)**, 37-41 (2011)
6. Yıldırım K., Altun S. and Ulcay Y., DSC Analysis of Partially Oriented (Poy) and Textured Poly (Ethylene Terephthalate) Yarns, *Res. J. Chem. Sci.*, **1(9)**, 57-66 (2011)
7. Karthikeyan C.S., Wietasch H., Thelakkat M., Highly Efficient Dye Sensitized TiO<sub>2</sub> Solar Cells using Donor Antenna Dyes capable of Multistep charge Transfer Cascades, *Adv. Mater.*, **19**, 1091 (2007)
8. Kwar S.S., Chalcogenide Thin Films Having Nanometer Grain Size for Photovoltaic Applications, *Res. J. Chem. Sci.*, **1(8)**, 31-35 (2011)
9. Chen C.Y., Wang M., Li J.Y., Pootrakulchote N., Alibabaei N., Ngoc C.H., Decopper J.D., Tsai J.H., Gratzel C., Wu C.G., Zakeeruddin S.M. and Gratzel M., Highly efficient Light Harvesting Ruthenium sensor for thin film dye sensitized solar cell *ACS Nano* **3**, 3103 (2009)
10. Mishra A., Fischer M.K.R. and Bauerle P., Metal Free Organic Dyes for Dye sensitized solar cells, *Angew Chem. Int. Ed.*, **48**, 2474 (2009)
11. Ito S., Zakeeruddin S.M., Hummphy R. - Baker, Liska P., Charvet R., Comte P., Nazeerudin M.K., Pechy P., Takata M., Miura H., uchida S. and Gratzel M., Highly Efficient organic Dye sensitized solar cells controlled by Nano-crystalline-TiO<sub>2</sub> Electrode thickness, *Adv. Mater.*, **18**, 1202 (2006)
12. Zhang G., Bala,H. Cheng Y., Shi D., Lv X., Yu Q. and Wang P., High efficiency and stable dye sensitized solar cell with organic Chromophore featuring a binary n-conjugated spacer, *Chem. Commun.*, 2198 (2009)
13. Roy M.S., Balaraju P., Kumar Manish and Sharma G. D., Dye sensitized solar cell based on Rose Bengal dye and nanocrystalline TiO<sub>2</sub>, *Solar Energy Materials and Solar Cells*, **92**, 909 (2008)
14. Zazeeruddin M.K., De Angelis F., Fantae S., Selloni A., Viscardi G., Liska P., Ito S., Bessho T., Gratzel M., *J. Am. Chem.Soc.*, **127**, 16835 (2005)
15. John A. Mikroyannidis, Minas M. Stylianakis, Suresh P., Roy M.S. and Sharma G.D., Synthesis of perylene monoimide derivative and its use for quasi-solid-state dye-sensitized solar cells based on bare and modified nano-crystalline ZnO photoelectrodes, *Energy and Environment Science*, **2**, 1293 (2009)
16. Thirumaran S. and Sathish K, Molecular Interionic Interaction Studies of Some Divalent Transition Metal Sulphates in Aqueous Ethylene Glycol at Different Temperatures, *Res. J. Chem. Sci.*, **1(8)**, 63-71 (2011)
17. Ozuomba J.O. and Ekpunobi, A Sol-Gel Derived Carbon Electrode for Dye-Sensitized Solar Cells, *Res. J. Chem. Sci.*, **1(8)**, 76-79 (2011)
18. Nazeeruddin M.K., Kay A., Rodicio I., Humphry-Baker R., Müller E., Liska P., Vlachopoulos N., Grätzel M., Conversion of light to electricity by cis-X<sub>2</sub>bis(2,2'-bipyridyl-4,4'-dicarboxylate)ruthenium(II) charge-transfer sensitizers (X = Cl-, Br-, I-, CN-, and SCN-) on nanocrystalline titanium dioxide electrodes, *J. Am. Chem. Soc.*, **115**, 6382 (1993)
19. Sharma G.D., Choudhary V.S., Janu Y. and . Roy M.S Mechanism of charge generation and photovoltaic effects in lead phthalocyanine based Schottky device., *Material Science, Poland*, **25** 1173–1191 (2007)
20. Ito S., Liska P., Comte P., Charvet R.L., Pechy P., Bach U., Schmidt-Mende L., Zakeeruddin S.M., Kay A., Nazeeruddin M.K., Grätzel M., Control of dark current in photoelectrochemical (TiO<sub>2</sub>/I<sup>-</sup>-I<sub>3</sub><sup>-</sup>) and dye-sensitized solar cells, *Chem. Commun.*, **4351** (2005)
21. O'Regan B.C., Durrant J.R., Sommeling P.M. and Bakker N.J., Multistep Crystal Nucleation: A Kinetic Study Based on Colloidal Crystallization, *J. Phys. Chem.*, C **111**, 14001 (2007)
22. Li Y., Cao Y., Gao J., Wang D., Yu G. and Heeger A.J., Electrochemical properties of luminescent polymers and polymer light-emitting electrochemical cells, *Synth. Met.* **99**, 243 (1999)
23. O'Regan B.C., Scully S., Mayer A.C., Palomares E. and Durrant J., The Effect of Al<sub>2</sub>O<sub>3</sub> Barrier Layers in TiO<sub>2</sub>/Dye/CuSCN Photovoltaic Cells Explored by Recombination and DOS Characterization Using Transient Photovoltage Measurements, *J. Phys. Chem.*, B **4616**, **109** (2005)
24. Tennakonne K., Jayaweera P.V.V. and Bandaranayake P.K.M., Dye-sensitized

- photoelectrochemical and solid-state solar cells: charge separation, transport and recombination mechanisms, *J. Photochem. Photobiol. A* **158**, 125 (2003)
25. Yu H., Zhang S., Zhao H., Will G. and Liu P., An efficient and low-cost TiO<sub>2</sub> compact layer for performance improvement of dye-sensitized solar cells, *Electrochim. Acta.*, **54**, 1319 (2009)
26. Halme J., Boschloo G., Hagfeldt A. and Lund P., Spectral Characteristics of Light Harvesting, Electron Injection, and Steady-State Charge Collection in Pressed TiO<sub>2</sub> Dye Solar Cells, *J. Phys. Chem. C*, **112**, 5623(2008)
27. Mikroyannidis John A., Suresh P., Roy M.S., Sharma G.D., Triphenylamine- and benzothiadiazole-based dyes with multiple acceptors for application in dye-sensitized solar cells, *J. Pow. Source* **195**, 3002 (2010)
28. Bajaraju P., Janu Yojana, Roy M.S. and Sharma G.D., Dye sensitized solar cells based on pyronine G dye and TiO<sub>2</sub>, *AIP Conf. Proceeding* **1004** 135- 140 (2008)